University of Nevada, Reno

Remediation of SR-89 in Emerald Bay, CA

A thesis submitted in partial fulfillment
of the requirements for the degree of

Bachelor of Science in Geological Engineering and the Honors Program

by

Cheyenne K. Lawrence, Kate Lynne R. Curtin, and Trevor L. Price

Dr. Robert Watters, Thesis Advisor

May, 2017

UNIVERSITY OF NEVADA RENO

THE HONORS PROGRAM

We recommend that the thesis
prepared under our supervision by

CHEYENNE KAY LAWRENCE

entitled

REMEDIATION OF SR-89 IN EMERALD BAY, CA

be accepted in partial fulfillment of the
requirements for the degree of

BACHELOR OF SCIENCE, GEOLOGICAL ENGINEERING

_____

Robert Watters, Ph.D., Thesis Advisor

_____

Tamara Valentine, Ph.D., Director, Honors Program

May, 2017

Abstract

Due to a combination of large tourist traffic and high geo-hazard risks, it is clear that SR-89 around Emerald Bay needs significant remediation. Occasional rock falls cover the road and reoccurring avalanches cause the road to be closed throughout winter. From late-January to mid-May, two methods of remediation were assessed. It was proposed that we could either construct a rock shed onto the current road to protect against the geo-hazards, or we could bypass the route altogether with a bridge over the mouth of Emerald Bay. The plausibility of both methods is tested based on shear and point load tests conducted on site-obtained samples. Although it was determined that both methods were plausible, our conclusion is that the bridge is a more feasible method based on the ability to widen the road during and after construction.

Acknowledgements

For Bob,

The never-ending supply of thoughtful guidance and Scottish humor preserved our sanity and enriched our academic careers.

Table of Contents

List of Tables

List of Figures

List of Illustrations

Introduction

The beauty of Emerald Bay is unrivaled. Whether it be the crisp evergreen pines that line the slopes around it, the historic Vikingsholm and tea house that stand admirably within it, or the crystal clear emerald water that fills it, it is abundantly apparent that Emerald Bay is something that should be treasured. It is unfortunate, however, that the extreme beauty of the bay is in constant contrast with the road that surrounds it. The road, SR 89, that arches around the bay does not reflect the same beauty as the glistening water below. Any who have travelled to Emerald Bay, whether local or tourist, can comment on how compact, winding, and unsafe much of the road is. During the warmer months, much of the road is prone to rock falls, with one section of it being primarily formed from landslide deposits. During the colder months, the road remains closed due to snow and avalanche danger. Both of these issues, along with the knowledge that this road receives large amounts of traffic that oftentimes fills up both shoulders of the road and all parking lots in the area, indicate that a solution is needed. In the early 1960s, Caltrans created a written report on this very issue and listed several solutions to the SR-89 problem. These solutions can be limited down to two plausible project designs. The first involves the implementation of a bridge across the mouth of the bay. This would bypass the hazardous path that follows the mountain side around the bay. The second option would be to rework the existing road into a wider road covered by several snow and rock sheds to protect against avalanches and rock falls. Both of these options would enable the road to be open year-round and limit the danger to locals and tourists who frequent the road. Although these plans were struck down in the 1960s due to opposition from the public, it is our desire to test the plausibility of these two options and discuss the possible

implementation of them in a way that would retain or add to the natural beauty of Emerald Bay and its surroundings.

Site of Interest

Our site of interest is a well-known tourist attraction visited by hundreds of thousands of people each year. If Lake Tahoe is the magnificent crown sitting upon the sierras, then Emerald Bay is the crown's most beautiful embedded emerald. When faced with even just a few pictures of this beautiful bay, it isn't hard to see the comparison.

Illustration 1**:** Emerald bay during a colorful sunset (emeraldbaylodge.com, 2017)

Illustration 2: Emerald bay covered in snow (usda.gov, 2017)

Emerald Bay and its crystalline waters are a beautiful sight in summer, winter, and everything in-between—something I think the above images can attest to. I feel as though Illustration 2 conveys one of the reasons why an all-weather route is needed. That, however, will be addressed more completely further into the report. Currently, we will focus on how this bay formed and what its geological history can tell us about our project.

Glacial Activity

Emerald Bay, and Tahoe for that matter, were formed due to glacial activity. The glaciers slowly pushed through the high Sierras, rearranging the topography and geology as they continuously thawed and reformed (CA Conservation). This thawing and refreezing happened roughly four to six times, each time changing the peaks and valleys of the Sierras (CA Conservation). Some of the most recent glaciers were the Tioga Stage and the Tahoe Stage, which were 20,000 and 160,000 thousand years ago, respectively (CA Conservation). This erosion process created by the glaciers causes a large amount of sediment deposit. This sediment deposit, or glacial till, is one of the primary make-ups of Emerald Bay. Addressing Emerald Bay's formation in a more specific manner, a roughly four-mile-long glacier formed on the north side of Dick's Peak and made its way down eagle creek and into Tahoe, leaving much of its collected deposits in Emerald Bay as it receded (CA Conservation). Fannette Island, famous for the tea house that was built on it, was also formed during all of this. As the glaciers receded, they eroded away the rock surrounding the island leaving only the more resistant rock of the island left (CA

Conservation). formations like this are termed roche moutonee, which translates to sheep rock (CA Conservation).

Geologic Units

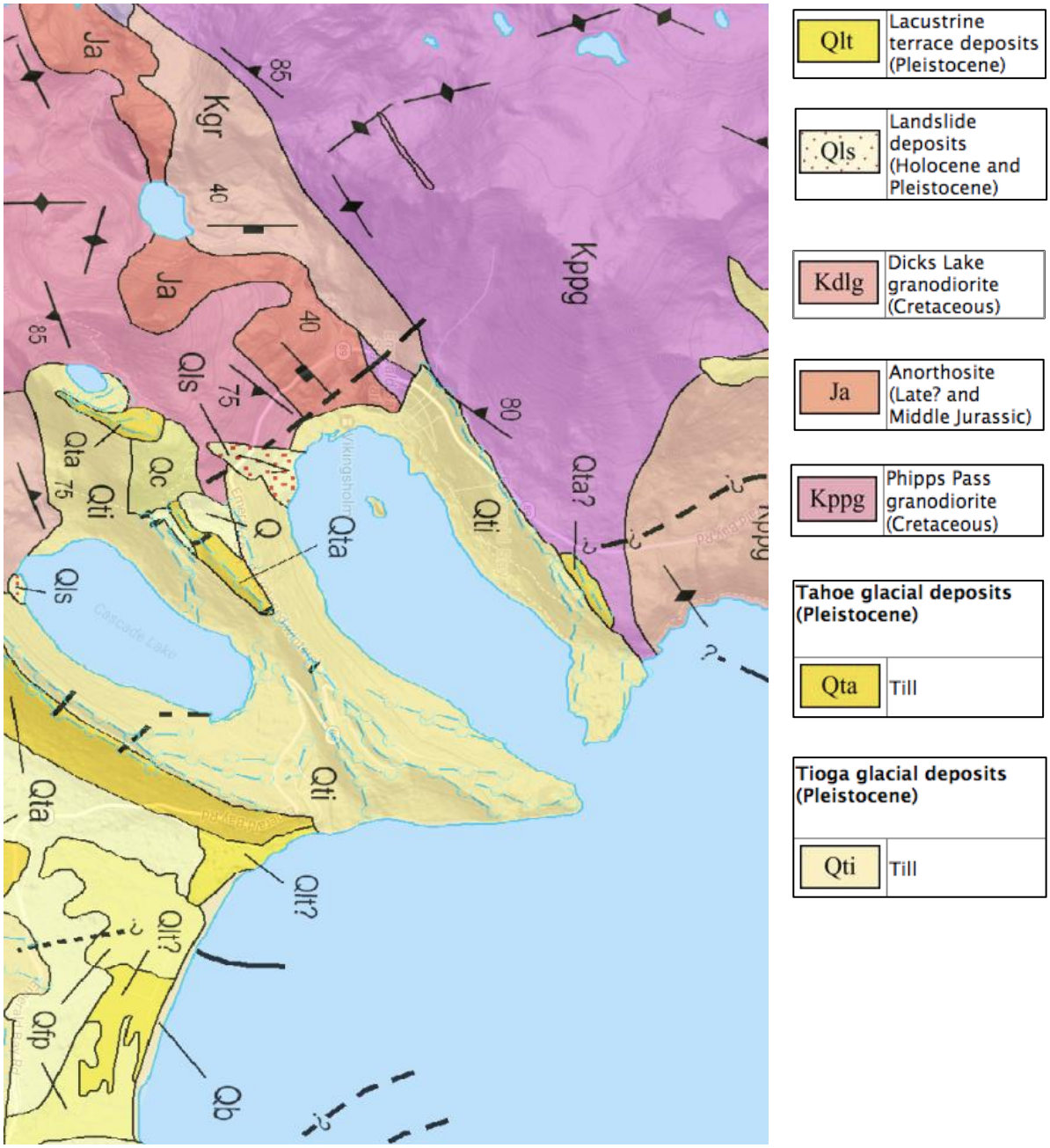

Figure 1: Geologic map of Emerald Bay. (State of California, Department of Agriculture)

The most important geologic units will be the Qls and Qti as both of those compose the area of and pose a danger to our two mitigation projects. In regards to the plan that attempts to remediate the existing road, Qls with be the most important geologic unit. As the description states Qls are deposits from landslides. If you look at the geologic map (Figure 3), you'll notice that SR 89 runs right through the Qls geologic unit. Using general intuition, it is easy to conclude that this is an area prone to rock falls and landslides, which pose a danger to the road. This will be discussed further in the report. The road runs through many other layer, all of which must be addressed—but none is more or a hazard to this project than Qls. In regards to the plan that involves building a bridge across the mouth of Emerald Bay, the Qti geologic unit will be the most important to address. As the description stated, Qti is till from the Tioga glacial deposits. As the Tioga glacier receded it left copious amounts of ground down sediment within most the bay. Our job will be to test this sediment and the layers beneath it to determine if it capable of withstanding a heavily traveled bridge. As you've seen, the geology of Emerald Bay is relatively simple, consisting mostly of till from the various glaciers that formed it. The simplicity of the surrounding geologic units shouldn't take away from the fact that there are hazardous components in the area that show both the necessity and difficulty of the proposed projects.

Rock Fall/Slide Hazard

Illustration 3: A C.W. Vernon Photo that shows the reconstruction process after a significant Emerald Bay rock fall.

Within Lake Tahoe, SR 89 around emerald bay has the most significant Rock fall/slide hazard and continues to pose problems to this very day. Some of the significant examples are listed in an article by Cooper and O'Rourke (1974). Although the article is dated, it provides several important examples that put the Rockfall/slide hazard in perspective. Documented was a slide that occurred in 1952 along SR 89. Further into the

article they discuss a second slide that occurred in the winter of 1955-1956. This landslide deposited over 200,000-cy of material onto the road and down into the bay. The scarp of this landslide it still visible to this day. It goes without saying that the reconstruction process was long and costly and ultimately ended with the death of one worker. It was this landslide that created the initial discussion for the bridge and rock/avalanche sled remediation methods that this report is presenting. IT is highly likely that these landslides are connected to the avalanche threat in the area (Cleaves et. al, 1960). There was no one to directly witness the above-mentioned landslides but from the lack of a slump scarp and the fact that it occurred in winter, it would be correct to assume that it was an avalanche induced landslide (Cleaves et. al, 1960). As the landslide traveled down the slope, it seemed to be redirected by a sturdy "rock island" that exists above and below the highway (Cleaves et. al, 1960). At the time of the 1960 report, this rock island was weakened and could pose a danger if another large-scale landslide occurred (Cleaves et. al, 1960). It would be incorrect, however, to assume that landslides and rock falls are a thing of the past. Just last year on February 19, 2016, a Rockfall shut down the road for several hours until construction workers could clear the debris off the road. The Rockfall hazard will be assessed and visualized further in this report.

Avalanche Hazard

Illustration 4: SR-89 during a typical winter. (Emerald Bay State Park, 2017)

Being located in Lake Tahoe, one of the snow sports capitals of the world, it is easy to understand how avalanches can be a significant risk to Emerald Bay. At any point during winter, Emerald Bay can have upwards of 30 feet of snowfall along SR 89. This, in addition to the vertical slopes that surround it, make avalanches nearly inevitable. Luckily, these avalanches don't pose a significant threat to humans. This isn't, however, because they don't contain the necessary power and occurrence rate to endanger human life, but instead because SR 89 is closed for nearly the entirety of the winter every year.

As we move forward in making SR 89 an all-weather route, we must design for the risk that avalanches will pose.

Methods of Mitigation

This portion of the report will focus primarily on mitigating the existing road, SR 89, into a safe all weather route. Other options that involve creating an entirely different road-way will be addressed elsewhere in the report. The first method that will be discussed is the implementation of snow and rock sheds along the roadway. The second method of mitigation is the construction of a tunnel through the landslide and avalanche area. Both options come with their pros and cons and will be delved into extensively below. An important part of these mitigation methods is the extensive widening of the current roadway. Since Emerald Bay is an impressive beauty that people travel for miles to see, it isn't surprising that on any given day a plethora of vehicles are seen parked along the sides of the roads. This creates a hazard for drivers and bicyclists, as the road is tight and windy to begin with. Widening the road will somewhat alleviate this hazard and allow for a safer visit for tourists. The following image shows the parking on an average day.

Illustration 5: The above image shows the overflow of parking that occurs around Emerald Bay on any given day. (Google Maps, 2017)

The above image is taken from Google Maps in the widest section of SR-89 around Emerald Bay. The average width is much smaller, yet still accompanies the same overflow parking along the sides of the road. Ideally, the construction of an extra parking lot would alleviate this hazard, but due to the lack of open spaces in the area, it isn't currently possible. As stated above, we will instead focus on widening the current road. Below is the original before and after of SR 89 presented in the 1960 report.

Illustration 6: The image shows the current route of SR-89. (State of California, Division of Highway)

Illustration 7: The image to the right shows an example of the route after completion of the project. (State of California, Division of Minerals)

Rock Shed Method of Mitigation

In the original 1960s report, one of the proposed methods utilized the technology of rock and avalanche sheds to make the existing SR 89 route around Emerald Bay a safe and all weather route. The idea is to cover most of SR 89 in a snow shed to divert both snow and rock from the roads. From a design aspect, Japanese techniques would be applied to this environment to ensure quality design. Rock sheds have been used extensively throughout the compact roads of Japan and would transition well to this environment.

Rock Shed Versus Other Mitigation Methods

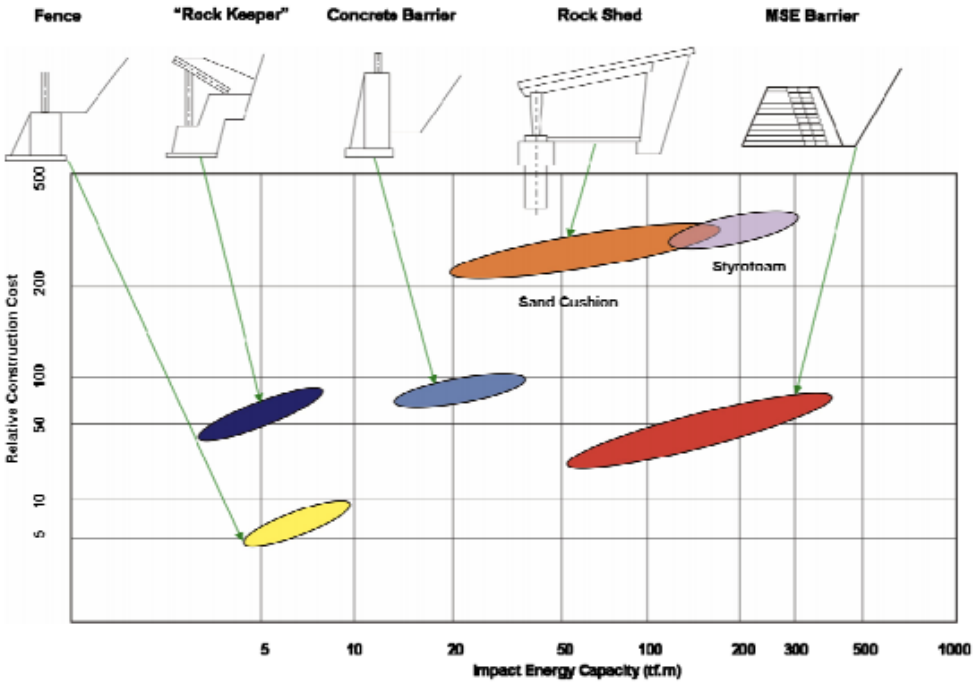

Figure 2: The above image compares the construction cost and impact energy capacity of various rock fall mitigation methods. (Hiroshi et al., 2007)

As shown in the previous image, the construction costs are incredibly high for rock sheds, but also have some of the highest impact energy capacity as compared to the other models. The only exception being the MSE barriers, which wouldn't mitigate the rock fall/landslide hazard of Emerald Bay. The fact that such a large-scale landslide has occurred and may again occur in Emerald Bay means that it would be safer and less damaging to divert the landslide over the highway further downslope, rather than putting up a MSE barrier to stop it at the level of the highway.

Cushion Layer

One of the most effective components of rock sheds is the thin cushion layer that is installed on top of most rock sheds. The cushion layer acts to dampen the impact energy received from rock falls. There are two main factors that are essential in cushion design and, for that matter, rock shed designs. These factors are the weight impact force and the transmitted impact force, as shown in the image below.

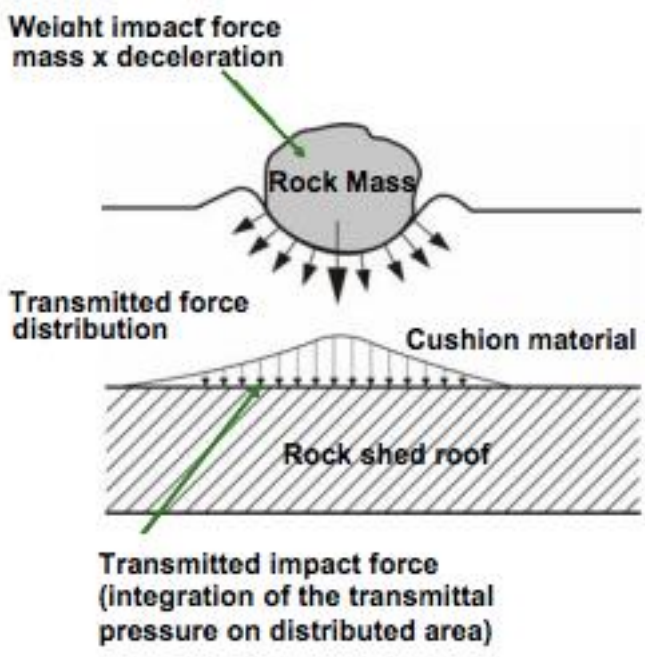

Figure 3: The image to the left shows the relationship between the rock mass and the shed roof. (Hiroshi et al., 2007)

Due to the cushion layer, the impact of the rock onto the cushion is not equal to the force that is received by the rock shed roof (Hiroshi et al., 2007). In plain terms, the impact from the rock mass is dispersed through the cushion layer, into the rock shed roof, and back into cushion layer, propagating throughout the cushion layer like a wave (Hiroshi et al., 2007). The most important aspect to determine is the relationship between the weight impact force and the transmitted impact force. The roof itself can be visualized as a fixed elastic one-dimensional structure. This, of course, is an over

simplification, but can give us an estimate of how force travels through the layer using the stress transfer theory. The image below illustrates this.

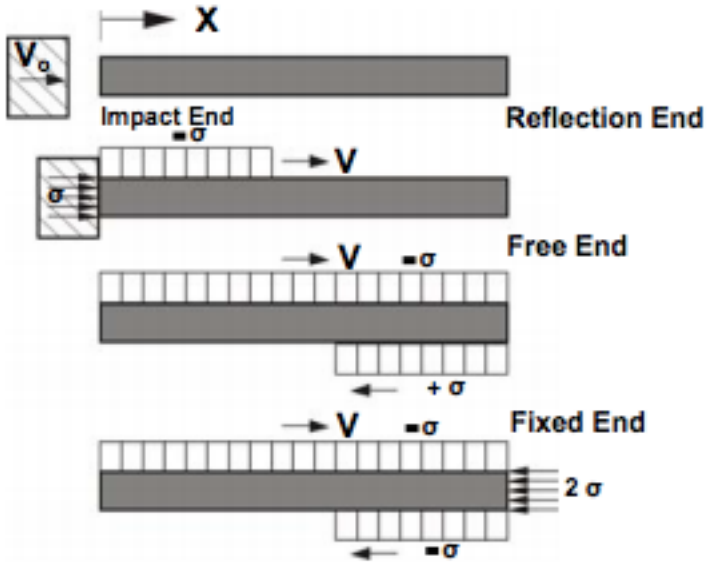

Figure 4: The above image illustrates the transmission of impact stress through both a free and fixed end elastic bar. (Hiroshi et al., 2007)

For the fixed end bar, the impact stress is reflected with the same magnitude and sign. Relating this back to a rock shed roof, the transmitted impact force would be twice the weight impact force. This, of course, is the relationship if a cushion layer is not present in the design. When a cushion layer is factored in, there isn't such a linear relationship between the weight impact force and the transmitted impact force. The implementation of a cushion layer breaks down the stress transfer theory and makes the transmitted force in-between 1 to 2 times the weight force (Hiroshi et al., 2007). When designing rock sheds and cushion layers, an empirical equation is used to determine the

transmitted impact. The equation used is shown below and is taken from the Japanese Rock Fall Protection Measures Handbook (2000).

$$P = .02(mg)^{2/3}\ \lambda^{2/5}\ H^{3/5}\ \beta$$

The above equation is an empirical equation that indicates the design impact force. The variables are as follows:

$m = mass\ (kg)$

$g = gravity\ (\frac{m}{s^2})$

$\lambda = Lame's\ parameter\ for\ cushion\ material\ kN/m^2$

$H = height\ (m)$

$\beta = (\frac{T}{D})^{-.58}\ \ ,\ \ where\ T\ is\ cushion\ thickness\ and\ D\ is\ rock\ diameter$

This equation is, of course, only one of many similar equations that have been derived to calculate the design impact force. However, since this report has a subtle emphasis in applying Japanese techniques to the United States, it will be the equation used when calculating the design impact force.

Cushion Material

Another important aspect to consider when designing a rock shed cushion layer is the material you want to use. Sand is the most typical material used as cushion layers because it is cheap and somewhat effective. For example, a 200-kg rock mass with diameter of 0.5m impacting a 0.9m thick sand cushion layer ($\lambda = 1000\ kN/m^2$) from a height of 50m would give an impact force as follows:

$$P = .02(mg)^{2/3}\ \lambda^{2/5}\ H^{3/5}\ \beta$$

$$P = .02(200kg \times 9.81m/s^2)^{2/3}\ (1000kN/m^2)^{2/5}\ (50m)^{3/5}\ (\frac{.9}{.5})^{-.58}$$

$$P = 369.4\ kN$$

As you can see above, sand does a sufficient job limiting the transmitted impact force that is received by the rock shed roof. This can, of course, be improved upon. Many companies are beginning to use Styrofoam as a more efficient cushion layer material.

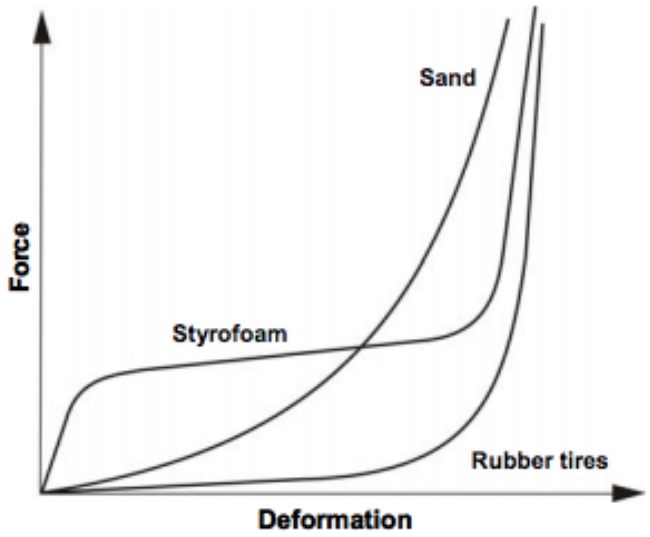

Figure 5: The above image compares the three most used cushion materials in regards to their deformation from force. (Hiroshi et al., 2007)

As the above image indicates, Styrofoam has a much better initial deformation to force than the other two materials. The greatest consequence of using Styrofoam as a material is that once it is compacted, any subsequent rock falls will transfer their full force to the rock shed roof (Hiroshi et al., 2007). As such, the cushion layer would need to be maintained regularly. It does, however, lower the design impact force significantly. This is because a larger cushion layer can be used. Sand is typically limited to .9 meters to minimalize the weight applied to the top of the rock shed. Since Styrofoam weighs a considerable amount less, a thicker cushion layer can be used. For example, below is the same example as above except with a cushion thickness of 3 meters and an estimated λ of $750\ kN/m^2$.

$$P = .02(mg)^{2/3}\ \lambda^{2/5}\ H^{3/5}\ \beta$$

$$P = .02(200kg{\times}9.81m/s^2)^{2/3}\ (750kN/m^2)^{2/5}\ (50m)^{3/5}\ (\frac{3}{.5})^{-.58}$$

$$P = 163.8\ kN$$

By increasing the thickness of the cushion, we can decrease the design impact force by 44%. It must be noted, however that the use of Styrofoam comes with a greater cost. Both the base material and the maintenance cost are more than what the cost would be for a sand cushion.

Typical Rock Shed Design

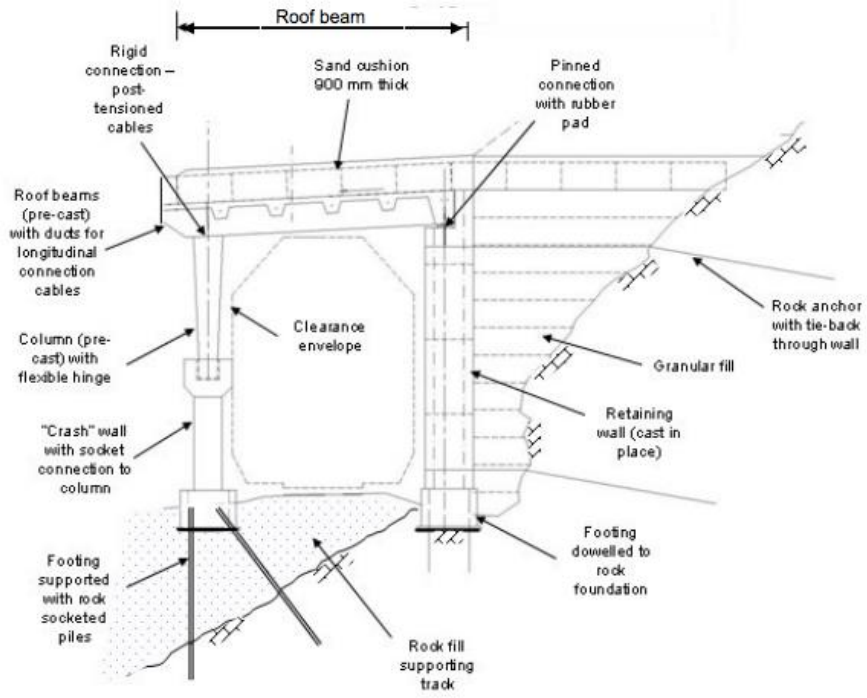

Figure 6**:** A typical cross section of a rock shed. (Hiroshi et al., 2007)

The above cross section shows the basic parts of a rock shed. On the top, a .9m sand cushion is modeled. Some important aspects to note are that the rock shed is bolted to the rock face. This means that the rock face must have strength testing done on it. It is not uncommon for the outer rock masses to be bolted to more secure rock masses beneath them and then bolted to the rock shed. This ensures more stability in the model. Another important aspect to note is that the rock shed uses socketed piles that are usually connected to the rock foundation below the roadway.

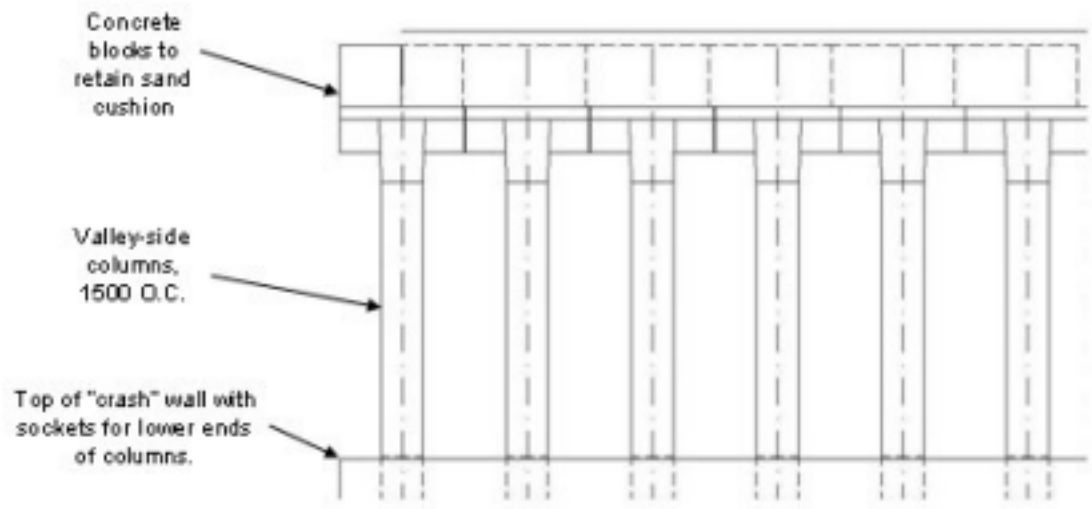

Figure 7: Shows a view of the columns that support the rock shed roof. (Hiroshi et al., 2007)

Three main components of the rock shed are viewable in the image above. Starting at the top, we can see the concrete blocks used to keep the cushion material stationary. The greater the angle applied to the rock shed roof, the more stress these blocks must support. Valley-side columns are the columns that need to be able to support

the roof on the side of the shed that isn't facing the rock cliff. These are usually made of concrete (Hiroshi et al., 2007). An interesting design consideration is the creation of a crash wall along the length of the rock shed. This wall would have to be able to withstand the horizontal impact of a car. The wall serves as protection for the columns to ensure that the rock shed remains intact. All the components in a rock shed need to be considered and designed for based upon the expected impact force.

Snow Considerations

When constructing a rock shed in winter terrain, the dynamics of snow need to be accounted for. This involves assessing both the expected dead weight of snow on the shed and also the potential for avalanches. If avalanches are considered to be plausible, then the stress that they exert on the roof of the rock shed need to be considered. The following equation is derived by Briukhanov, A.V. et al. and is used to estimate the stress of an avalanche on an object.

$$P = \rho v^2 a^2 \frac{800m(1+m)}{(1+800m)^2}$$

$\rho = density\ of\ snow$

$v = velocity$

$a = 1\ for\ maximum\ stress$

$m = mass\ ratio\ of\ air\ to\ ice$

Emerald Bay Rock Shed

One of the first aspects that needs to be considered is the design impact force. This will be calculated using the equation below:

$$P = .02(mg)^{2/3}\ \lambda^{2/5}\ H^{3/5}\ \beta$$

To use the above equation, an average rock fall must be estimated. The image below will help in estimating the potential rock fall size.

Illustration 8: Project Site Slope, Emerald Bay. (Google Maps, 2017)

Just by using the above image we can get a general size of the rock falls that could occur. For the purposes of this project an average diameter of 2 meters will be used with a fall height of roughly 50 meters. Using the volume and an average density of granite ($2750\ kg/m^3$) we can calculate the mass as 8639.38 kg. A sand layer will be used in this project with a thickness of .9 meters. The equation is calculated as follows:

$$P = .02(mg)^{2/3}\ \lambda^{2/5}\ H^{3/5}\ \beta$$

$$P = .02(8639.38kg \times 9.81m/s^2)^{2/3}\ (1000kN/m^2)^{2/5}\ (50m)^{3/5}\ (\frac{.9}{.5})^{-.58}$$

$$P = 4547.7\ kN$$

Now that we have the design impact load the next step is analyzing the dimensions of the shed. To do this, we first have to know where it is located and how long it will be. The below image displays the projected project site and length of shed.

Illustration 9: Projected project site and length of rock shed. (Google Maps, 2017)

Although it isn't labeled directly in the image, the measured length is roughly 300 meters. After a widening of the road, the expected width of the roof would be roughly 10 meters. This makes for a total area of 3000 m^2. Using this, we can calculate the stress applied to the rock shed roof. This would make the stress applied to the roof 1.52 kN/m^2. Thus, for every meter squared of roof, a force of 1.52 kN must be designed for. In addition to this, the weight of the cushion layer must be accounted for. Using a density of 1600 kg/m^3 and multiplying by the acceleration of gravity ($9.81 m/s^2$) results in 15.7 kN/m^3. Multiplying this by the height of the cushion layer (.9 meters) results in a stress of 14.13 kN/m^2.

Snow Design

When considering the design aspects of making this an all-weather route, the stress of snow must be considered. The weight of snow can vary greatly depending on how wet and compacted it is. For this project, an average value of $2.357\ kN/m^3$ will be used. Multiplying this be an average snow fall of 6.1 meters' results in a stress of $14.37\ kN/m^2$. In addition to the dead load of snow, avalanche stress needs to be factored in. The calculations for estimating the stress received by the rock shed roof are listed below:

$$P = \rho v^2 a^2 \frac{800m(1+m)}{(1+800m)^2}$$

$$P = (.1g/cm^3)(30m/s)^2(1)^2 \frac{800(.12)(1+.12)}{(1+800(.12))^2}$$

$$P = 1.03atm = 104.37\ kN/m^2$$

For the above calculation, the following assumptions were made:

$\rho = .1g/cm^3$

$a = 1$

$v = 30m/s$

$m = .12$

In conclusion, the rock shed needs to be designed to withstand a total stress of $134.4\ kN/m^2$. This number is a combination of the stresses caused by the impact of rock falls and avalanches, as well as the weight of snow and the cushion layer. Essentially, this number is the total amount of force per square meter that the rock shed needs to support at any given time. Based on other projects, this is a reasonable stress for a rock shed to maintain against.

Field Reconnaissance

As the weather and conditions improved into mid-April, field reconnaissance was conducted at four areas of interest, particularly on the south side of the mouth of the bay and on the north end of the bay near the road and the trail to the Vikingsholm. The goal was to collect a topsoil sample and a fresh, unweathered sample of the granitic bedrock. Three soil samples and one rock sample were obtained from sites 1 and 2 but were omitted from the analysis due to the significant presence of organics in the soil and weathering in the rock sample. Two samples of air-dried sandy soil and 18 samples of unweathered granodiorite were obtained from sites 3 and 4. Descriptions of the samples and their testing parameters are given in the section “Testing Methods and Results”. An aerial view of the visited sites is given below:

Illustration 10: Aerial View of Sites Visited (Google Earth, 2017)

Testing Methods and Results

Point Load Index

This geotechnical method is used to classify the strength of a rock mass and its possible applications in geotechnical and soils engineering. The test is conducted by placing a rock specimen between two coaxial, conical platens and applying an increasingly larger concentrated load until the specimen fails by fracturing. The load at the point of failure is used to calculate the point load strength index. This value can then be used to classify the strength of the rock, most notably by using the uniaxial compressive strength. Point load index tests are often used in place of a uniaxial compression test for a number of reasons, the primary one being that point load index tests are a quicker and cheaper method of determining the integrity of a rock. They are

convenient for conducting tests in the field as the apparatus can be transported without much difficulty. Conducting these tests in the field can reduce the amount of time and money spent on more expensive compression tests in the laboratory and can provide prompt and efficient results on the integrity of field samples.

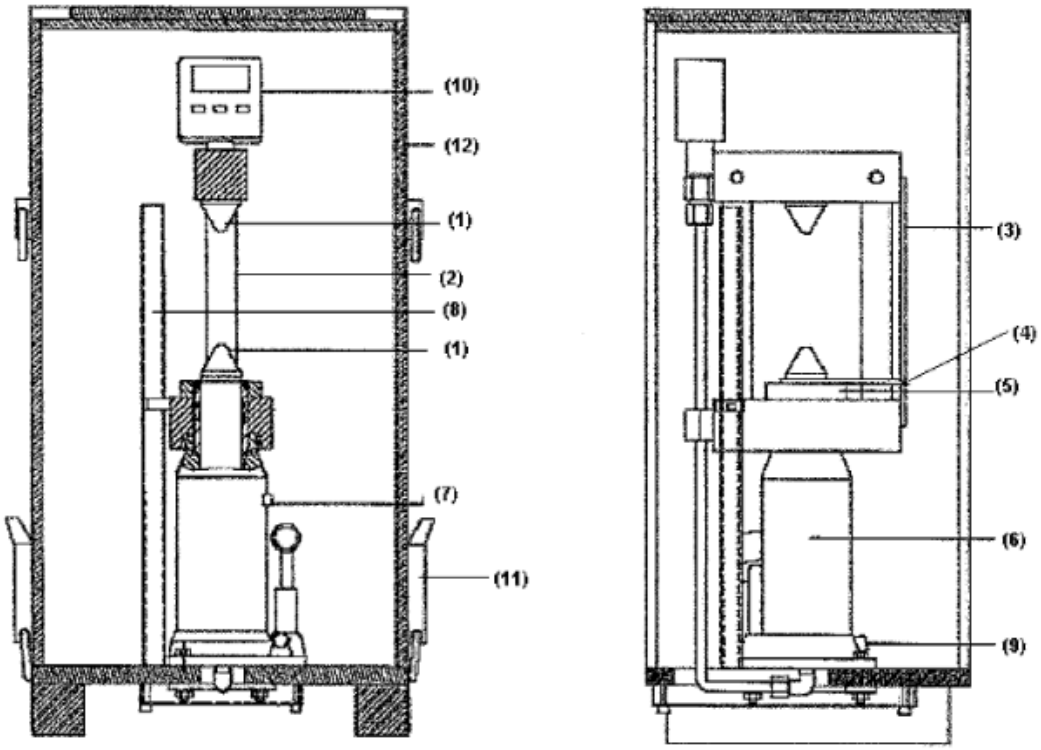

NOTE—Load frame general information (figure 1)Load is applied to the specimens through two standard hardened points (1)Two column fixed crosshead frame (2)Scale (3)Scale pointer (4)Attached by a bolt (5) to the hydraulic pump body (6)Oil filler cap (7)The hydraulic piston assembly incorporated the oil reservoir, a single acting pump, pressure relief valve (9), and a handle (8)Pump handle (8)Pressure release valve (9)Case latched for top cover (10)Digital pressure readout (11)Point load tester top cover(12)

Figure 8: Point Load Strength Test Apparatus (ASTM D5731-08, 2016)

Specimens to be tested using the point load strength index test should be in the form of core (cylindrical rock samples), cut blocks, or irregular lumps that must be no less than 35 mm and no more than 80 mm in diameter with a preferred test diameter, or initial distance between the platens, being 50 mm. Minimal specimen preparation is required in this test and any effect of moisture within the sample can be neglected in the results.

Results from the test are analyzed by obtaining the magnitude of the stress at failure, the initial displacement between the two platen contact points prior to the start of each test, and the final displacement at the point of failure. ASTM D5731-08 recommends that at least ten samples of core/block be tested.

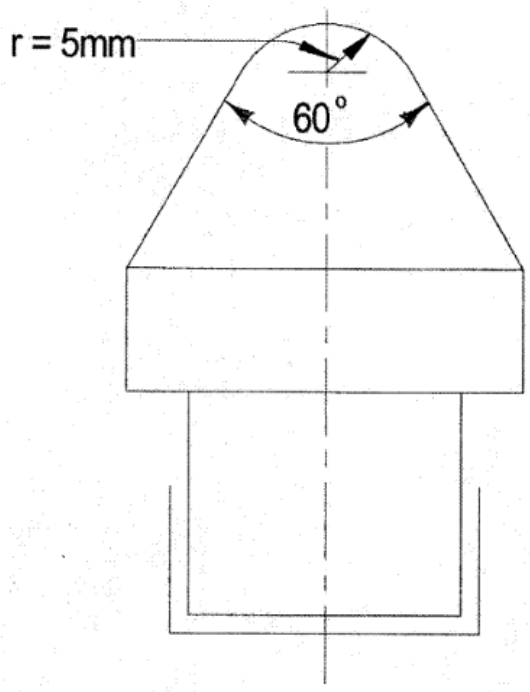

Figure 9: Schematic of Conical Platen for Point Load Test (ASTM D5731-08, 2016)

The samples from Emerald Bay largely consisted of granodiorite, a granitic rock containing plagioclase, quartz, and biotite. Granodiorite is a key component of the bedrock in the Tahoe region. Eighteen samples in total were tested using the point load method, with fourteen being retained for analysis (the two specimens with the highest stress values and the two specimens with lowest stress values were omitted from the data during processing). Each specimen was placed in between the conical platens of the apparatus and the platens were tightened using a hand pump until the specimen fit securely in between the platen contact points. The initial distance between the platens, D_e, was recorded using a ruler connected to the apparatus. The width of each specimen was not recorded during testing and, therefore, is assumed to be approximately 2 inches (50.8 millimeters).

Once the initial distance was recorded, the apparatus was cranked using the pump until the force acting through the platens and onto the specimen caused a failure in the rock (the rock fractured). The pressure at the point of failure was then obtained from a digital pressure readout and the final distance between the platen contact points was recorded. If the specimen slipped from the loading frame or did not otherwise fracture completely, the result was omitted and the test was repeated.

Once the initial distance, final distance, and stress at failure was recorded for each specimen, the loads at failure were calculated by multiplying the pressures at failure by the RAM area of the apparatus which is equal to 967.74 mm^2. From here, the uncorrected point load strength index was calculated for each specimen using the following formula:

$$I_s = \frac{P}{{D_e}^2} \quad \text{(MPa)}$$

Where I_s is the uncorrected point load strength index, P is the load in Newtons, and D_e is the initial distance between the platens.

In the case of testing large, irregular lumps like the samples of granodiorite, ${D_e}^2$ was calculated using: $\frac{4A}{\pi}$ where A is the cross-sectional area of the specimen.

Since the point load index varies as a function of D_e and the values for initial distance were not all the recommended 50 mm for block/irregular lump tests, a size correction factor must be applied to calculate a corrected point load index, $I_{s\,50}$. This correction factor equation varies depending on how close the specimen is to the 50-millimeter mark. For specimens that varied by more than 2 millimeters, the following correction factor equation was used:

$$F = \left(\frac{D_e}{50}\right)^{0.45}$$

For specimens that varied from the 50-millimeter mark by 2 mm or less, the following equation was used to account for the less significant error:

$$F = \sqrt{\frac{D_e}{50}}$$

Once these parameters are calculated, the uniaxial compressive strength can be determined for each sample by using the following equation:

$$\sigma_c = K * I_s$$

Where I_s is the uncorrected point load index and K is a generalized strength conversion factor which was taken to be 20 for our specimens.

Sample No.	De (mm)	Df (mm)	Width (mm)	Stress (Mpa)	Load (N)	Load (kN)	De^2	Is (Mpa)	Is (psi)	F	Is50 (Mpa)	σc
1	46.8	35	50.8	23.81	23041.89	23.04	2264.97	10.17	1475.50	0.97	9.87	203.46
2	51	47	50.8	14.11	13654.81	13.65	3041.53	4.49	651.14	1.01	4.53	89.79
3	47	42.5	50.8	16.06	15541.90	15.54	2750.32	5.65	819.60	0.97	5.50	113.02
4	60	49	50.8	10.61	10267.72	10.27	3170.96	3.24	469.64	1.09	3.51	64.76
5	46	42.5	50.8	16.8	16258.03	16.26	2750.32	5.91	857.37	0.96	5.69	118.23
6	49	44	50.8	12.82	12406.43	12.41	2847.39	4.36	631.95	0.99	4.31	87.14
7	51	48.5	50.8	26.27	25422.53	25.42	3138.60	8.10	1174.80	1.01	8.17	162.00
8	47.5	41	50.8	23.5	22741.89	22.74	2653.25	8.57	1243.17	0.98	8.38	171.43
9	48	41	50.8	15.54	15038.68	15.04	2653.25	5.67	822.08	0.98	5.55	113.36
10	53	49	50.8	18.3	17709.64	17.71	3170.96	5.58	810.03	1.03	5.73	111.70
11	50	46	50.8	10.44	10103.21	10.10	2976.82	3.39	492.25	1.00	3.39	67.88
12	49	45	50.8	14.64	14167.71	14.17	2912.10	4.87	705.63	0.99	4.82	97.30
13	47	44.5	50.8	9.83	9512.88	9.51	2879.75	3.30	479.12	0.97	3.21	66.07
14	53.5	50	50.8	16.77	16229.00	16.23	3235.67	5.02	727.46	1.03	5.17	100.31

Table 1: Point Load Test Data

Customary practice in analyzing point load strength test results is to plot the uncorrected point load index versus the uniaxial compressive strength. The result for the Emerald Bay data is given in the following plot:

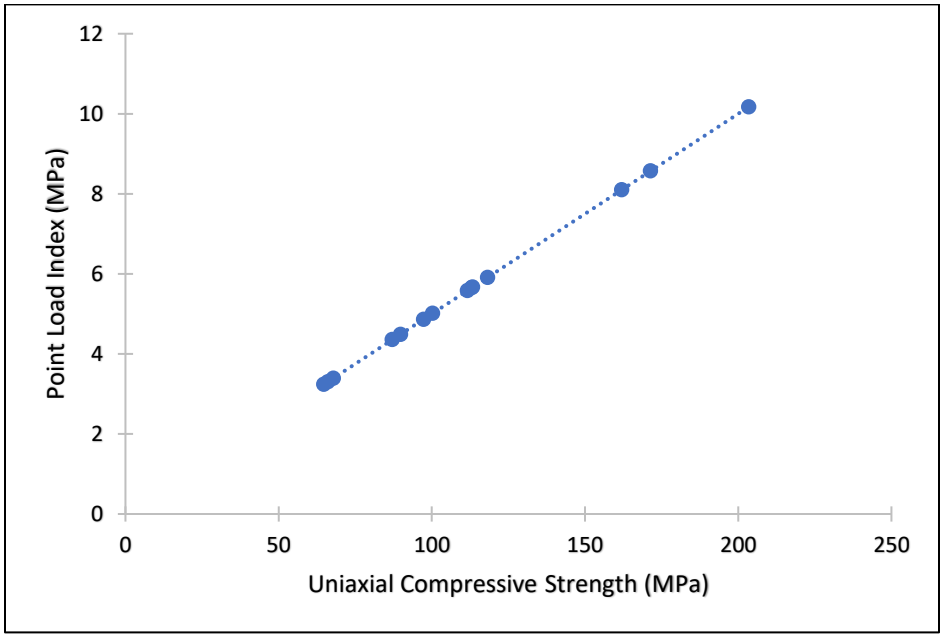

Figure 10: Plot of Uncorrected Point Load Index vs Uniaxial Compressive Strength

Based on the tabulated point load strength results, the average uniaxial compressive strength of the 14 specimens was calculated to be 112 MPa.

Description	Uniaxial compressive strength, MPa	Point-load strength index, MPa
Very high strength	> 200	> 8
High strength	100-200	4-8
Medium strength	50-100	2-4
Low strength	25-50	1-2
Very low strength	< 25	< 1

Table 2: Classification of Rock Material Based on Uniaxial Compressive Strength (Bieniawski, 1974)

Using the above table, the granodiorite bedrock in Emerald Bay can be classified as 'high strength'.

Another method of determining the integrity of the rock is taken from ASTM D5731-08 and given by the diagram below:

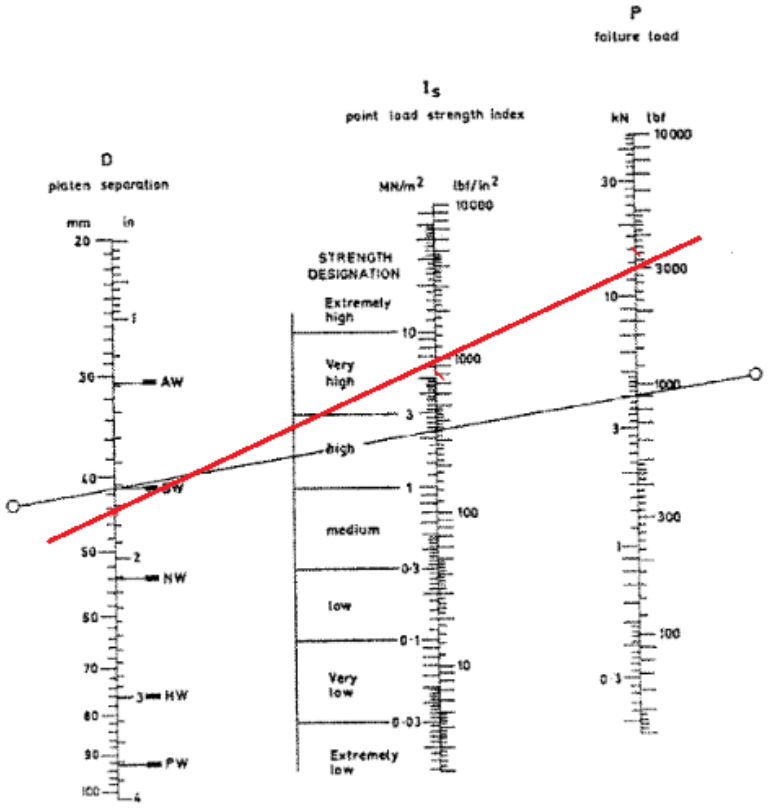

Figure 11: Descriptive Strength Classification of Rock (ASTM D5731-08, 2016)

This method was conducted by taking the averages of three parameters: the platen separation at failure, the uncorrected point load strength index (in pounds per square inch), and the failure load (in kN). Plotting these values on their respective scales and drawing a line of best fit yields a generalized strength classification for the rock material. The red line in the diagram above represents the data for the granodiorite samples, putting the bedrock material in to the ‘high’ to ‘very high’ range.

Based on the above strength classification results, the granodiorite bedrock in Emerald Bay would be considered suitable for the application of remediation measures on SR-89.

Direct Shear Test on Soil

This method is used to classify soils based on parameters such as the cohesion and the friction angle of the soil which have important effects on the integrity of a soil sample in geotechnical engineering. The test is conducted using a 2 inch x 2 inch shear box that holds a soil specimen during testing. The shear box is composed of two horizontal plates that slide past each other during testing, resulting in a shear stress on the soil. A schematic of the system is shown below:

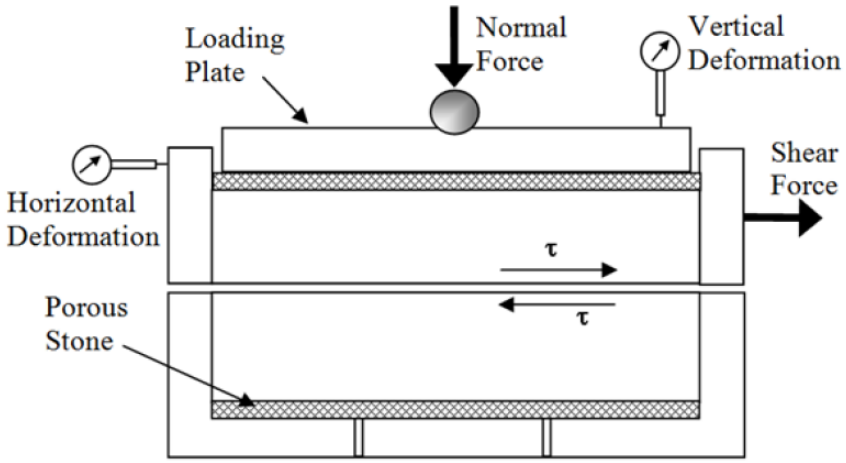

Figure 12: Direct Shear Testing Apparatus (IIT, 2017)

Horizontal displacement of the shear apparatus and shear load (in div) are collected during testing. Direct shear tests are run continuously until the shear load reaches a peak and settles into a residual stage.

The samples collected from Emerald Bay consisted of poorly-graded, dense, sandy soil with a high silica content. The sample was relatively dry at the time of testing so no oven-drying of the sample was conducted prior to testing. Three separate shear tests were conducted on fresh samples of the soil, each with an increased normal component. The statical relationship between the amount of weight (q) added to the machine and the normal force (N) acting on the specimen is given by the following equation:

$$N = 18.29 + 8q$$

The weights added for each of the three tests and their corresponding normal forces and normal stresses (using an area of 4 square inches) are given below:

Test	q (lb)	N (lb)	σ (psi)
1	8.8	88.69	22.17
2	17.65	159.49	39.87
3	26.5	230.29	57.57

Table 3: Values for Weight Added, Normal Force, and Normal Stress

The machine measures shear load (div) and displacement (1/1000 inch) and readings are taken every 30 seconds until residual shear is reached and a peak shear load is obtained. The shear loads must be converted to pounds by multiplying the initial load value by 0.276. From these data, the shear stress can be calculated using the area of the shear box (4 square inches) and the shear strain can be obtained by dividing the displacement by the total length of the shear surface (2 inches). The tabulated data are given in the following pages:

Time (s)	Shear Load (div)	Shear Load (lb)	Shear Stress (psi)	Disp. (in)	Shear Strain
30	0	0.00	0.00	0.00	0.00
60	0	0.00	0.00	0.00	0.00
90	7	1.93	0.48	0.00	0.00
120	22	6.07	1.52	0.00	0.00
150	57	15.73	3.93	0.00	0.00
180	91	25.12	6.28	0.00	0.00
210	128	35.33	8.83	0.00	0.00
240	151	41.68	10.42	0.01	0.00
270	168	46.37	11.59	0.01	0.01
300	180	49.68	12.42	0.02	0.01
330	190	52.44	13.11	0.03	0.01
360	202	55.75	13.94	0.03	0.02
390	215	59.34	14.84	0.04	0.02
420	226	62.38	15.59	0.04	0.02
450	234	64.58	16.15	0.05	0.02
480	247	68.17	17.04	0.06	0.03
510	253.5	69.97	17.49	0.06	0.03
540	261	72.04	18.01	0.07	0.03
570	269	74.24	18.56	0.08	0.04
600	275	75.90	18.98	0.08	0.04
630	277	76.45	19.11	0.09	0.04
660	280	77.28	19.32	0.10	0.05
690	282	77.83	19.46	0.10	0.05
720	256	70.66	17.66	0.11	0.06
750	290	80.04	20.01	0.12	0.06
780	288	79.49	19.87	0.12	0.06
810	290.5	80.18	20.04	0.13	0.07
840	292	80.59	20.15	0.14	0.07
870	292	80.59	20.15	0.14	0.07
900	289.5	79.90	19.98	0.15	0.08
930	288.5	79.63	19.91	0.16	0.08
960	288.5	79.63	19.91	0.17	0.08
990	285	78.66	19.67	0.17	0.09
1020	284.5	78.52	19.63	0.18	0.09
1050	281	77.56	19.39	0.19	0.09
1080	277	76.45	19.11	0.20	0.10
1110	274	75.62	18.91	0.20	0.10

1140	271.5	74.93	18.73	0.21	0.10
1170	273	75.35	18.84	0.22	0.11
1200	276	76.18	19.04	0.22	0.11
1230	275	75.90	18.98	0.23	0.12
1260	276	76.18	19.04	0.24	0.12
1290	276.5	76.31	19.08	0.25	0.12
1320	280	77.28	19.32	0.25	0.13

Table 4: Direct Shear Results for Test 1

Time (s)	Shear Load (div)	Shear Load (lb)	Shear Stress (psi)	Disp (in)	Shear Strain
30	6	1.66	0.41	0.00	0.00
60	27	7.45	1.86	0.00	0.00
90	70	19.32	4.83	0.00	0.00
120	132	36.43	9.11	0.00	0.00
150	183	50.51	12.63	0.00	0.00
180	221	61.00	15.25	0.01	0.00
210	248	68.45	17.11	0.01	0.01
240	265	73.14	18.29	0.02	0.01
270	289.5	79.90	19.98	0.03	0.01
300	308	85.01	21.25	0.04	0.02
330	328	90.53	22.63	0.04	0.02
360	340	93.84	23.46	0.05	0.03
390	354	97.70	24.43	0.06	0.03
420	370	102.12	25.53	0.07	0.03
450	383.5	105.85	26.46	0.07	0.04
480	397	109.57	27.39	0.08	0.04
510	409	112.88	28.22	0.09	0.04
540	419	115.64	28.91	0.10	0.05
570	435	120.06	30.02	0.10	0.05
600	448.5	123.79	30.95	0.11	0.06
630	462	127.51	31.88	0.12	0.06
660	473	130.55	32.64	0.13	0.06
690	482	133.03	33.26	0.13	0.07
720	494	136.34	34.09	0.14	0.07

750	501	138.28	34.57	0.15	0.08
780	508	140.21	35.05	0.16	0.08
810	509.5	140.62	35.16	0.17	0.08
840	514	141.86	35.47	0.18	0.09
870	517	142.69	35.67	0.18	0.09
900	521	143.80	35.95	0.19	0.10
930	512	141.31	35.33	0.20	0.10
960	514	141.86	35.47	0.21	0.11
990	521	143.80	35.95	0.22	0.11
1020	517	142.69	35.67	0.23	0.11
1050	520	143.52	35.88	0.24	0.12
1080	511	141.04	35.26	0.25	0.12
1110	508	140.21	35.05	0.26	0.13

Table 5: Direct Shear Results for Test 2

Time (s)	Shear Load (div)	Shear Load (lb)	Shear Stress (psi)	Disp. (in)	Shear Strain
30	16	4.42	1.10	0.00	0.00
60	50	13.80	3.45	0.00	0.00
90	87	24.01	6.00	0.00	0.00
120	139	38.36	9.59	0.00	0.00
150	195	53.82	13.46	0.00	0.00
180	237	65.41	16.35	0.00	0.00
210	283	78.11	19.53	0.00	0.00
240	325	89.70	22.43	0.00	0.00
270	360	99.36	24.84	0.00	0.00
300	381	105.16	26.29	0.00	0.00
330	395	109.02	27.26	0.00	0.00
360	419	115.64	28.91	0.01	0.00
390	444	122.54	30.64	0.01	0.01
420	463	127.79	31.95	0.02	0.01
450	485	133.86	33.47	0.02	0.01
480	503	138.83	34.71	0.03	0.01
510	522	144.07	36.02	0.03	0.02

540	547	150.97	37.74	0.04	0.02
570	560	154.56	38.64	0.04	0.02
600	575	158.70	39.68	0.05	0.02
630	592	163.39	40.85	0.05	0.03
660	610	168.36	42.09	0.06	0.03
690	616	170.02	42.50	0.06	0.03
720	630	173.88	43.47	0.07	0.04
750	647	178.57	44.64	0.08	0.04
780	660	182.16	45.54	0.08	0.04
810	672	185.47	46.37	0.09	0.04
840	683	188.51	47.13	0.09	0.05
870	684	188.78	47.20	0.10	0.05
900	697	192.37	48.09	0.10	0.05
930	704.5	194.44	48.61	0.11	0.05
960	706	194.86	48.71	0.12	0.06
990	712	196.51	49.13	0.12	0.06
1020	720	198.72	49.68	0.13	0.06
1050	723	199.55	49.89	0.14	0.07
1080	723.5	199.69	49.92	0.14	0.07
1110	722	199.27	49.82	0.15	0.07
1140	722	199.27	49.82	0.16	0.08
1170	733	202.31	50.58	0.16	0.08
1200	725	200.10	50.03	0.17	0.08
1230	727	200.65	50.16	0.18	0.09
1260	740	204.24	51.06	0.18	0.09
1290	731	201.76	50.44	0.19	0.09
1320	737	203.41	50.85	0.19	0.10
1350	740.5	204.38	51.09	0.20	0.10
1380	739	203.96	50.99	0.21	0.10
1410	737	203.41	50.85	0.22	0.11
1440	732	202.03	50.51	0.22	0.11

Table 6: Direct Shear Results for Test 3

Plotting the values of shear stress versus shear strain is customary for engineering practice and yields a series of curves that depicts the point of peak and residual shear stress for each test.

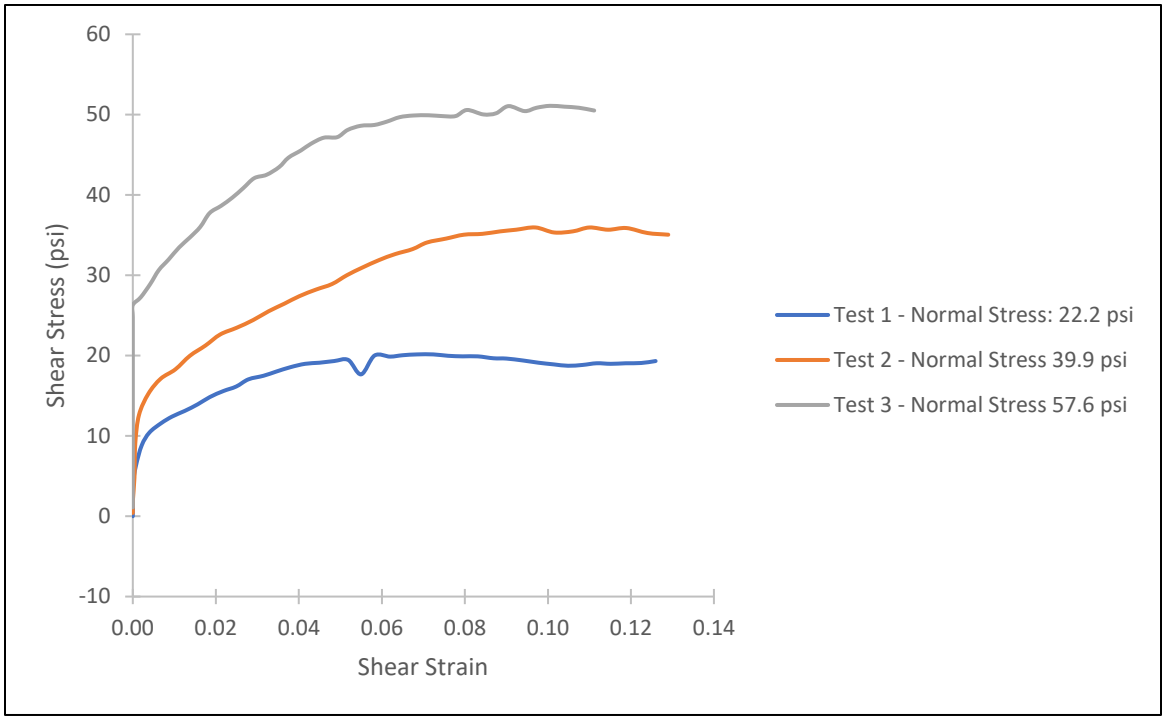

Figure 13: Plot of Shear Stress versus Shear Strain for Emerald Bay Soil

The results of this plot are indicative of a loose to medium-dense, sandy soil due to the lack of clear distinction between the peak shear stress and the residual shear stress.

A useful tactic in analyzing the geotechnical significance of a soil using the test data is to develop a Mohr-Coulomb Failure Envelope. This method is an effective way of determining the stability parameters of a soil, specifically the values for cohesion and friction angle. The Mohr-Coulomb relationship between shear stress and normal stress is given as follows:

$$\tau = \sigma tan\phi + c$$

Where τ is shear stress, σ is normal stress, ϕ is the friction angle, and c is the cohesion.

Using this relationship, a plot of the peak shear stress for each test versus the normal stress for each test can yield a Mohr-Coulomb Failure Envelope.

Test	Normal Stress (psi)	Peak Shear Stress (psi)
1	22.17	20.15
2	39.87	35.95
3	57.57	51.09

Table 7: Values of Normal Stress and Peak Shear Stress for Each Test

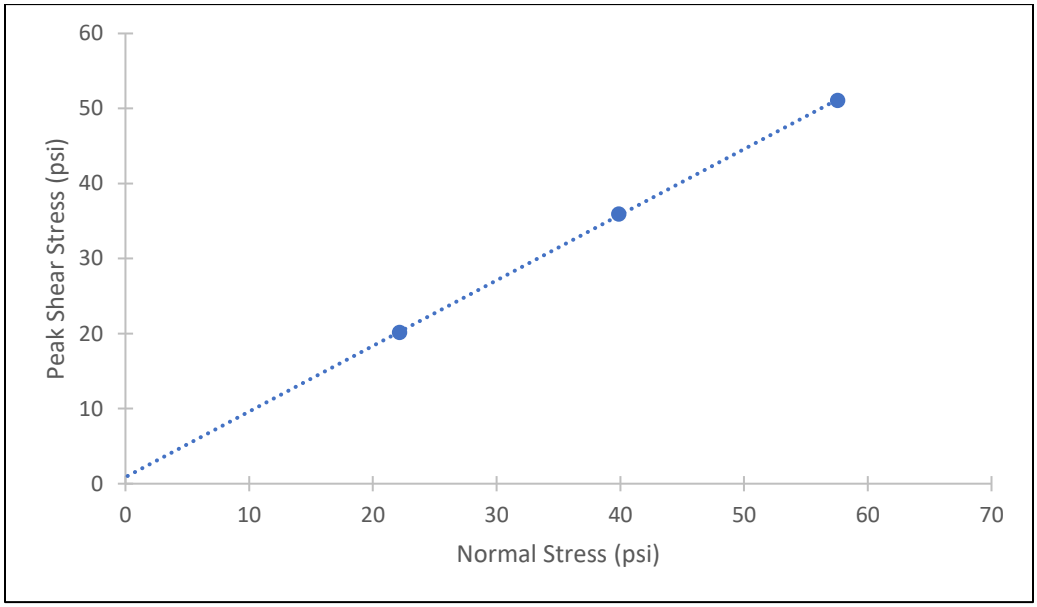

Figure 14: Mohr-Coulomb Failure Envelope

The linear relationship of the Mohr-Coulomb Failure Envelope can be used to determine the values of cohesion and friction angle for the soil. The y-intercept of the best-fit line of this plot is considered the cohesion value and the inverse tangent of the

slope of this line yields the friction angle. The results for the Emerald Bay specimen are given below:

Friction angle (ϕ)	Cohesion (c)
41.2°	0.87 psi

Table 8: Values for Friction Angle and Cohesion

The values above indicate that the specimen is a moderately-dense, minorly-cohesive sandy soil. Dense soils with little to no fine grains such as this specimen are likely to fail along a specific plane of weakness rather than fail by swelling as is often seen in cohesive, fine-grained soils. These parameters will need to be considered during the design process of remediation measures for SR-89.

Bridge Design

Case History

Due to constant road closures on the SR-89, that loops around Emerald Bay, the idea of constructing a bridge that crosses over the mouth of the bay will help keep the roads open year-round and even make travel time shorter for commuters as seen in Illustration 11.

Illustration 11: The proposed location and span of the Emerald Bay Bridge (Google Earth, 2017)

The plan for this bridge will be similar to the 1960 proposal, where the bridge will connect to roads on either side of the bay so vehicles do not have to travel around the mouth, where large amounts of snowfall, rockslides and avalanches are known to occur. Illustration 12 below is an image and sketch of the 1960 Emerald Bay Bridge proposal.

Illustration 12: Proposed 1960 Emerald Bay Bridge (Cleaves, 1960)

The proposal was rejected back in 1960 because the citizens that grew up around Lake Tahoe regarded Emerald Bay as a landmark of beauty and if a bridge were to be built, that beauty would be covered up and forgotten. Bridges are built to be aesthetically pleasing, decrease travel time, and to enhance the driving conditions for commuters. The original route, SR-89, to get around Emerald Bay is prone to high accumulation of snow, avalanches and even rockslides. This route also takes a great amount of time to get from one side of the bay to the other. Illustration 13 shows the commuters' route as of now.

Illustration 13: Route 89 around Emerald Bay (Google Maps, 2017)

The plan for the Emerald Bay Bridge is to make it an arch bridge, spanning roughly 1200 feet across the mouth of Emerald Bay. The proposed bridge will have similarities to the Vikingsholm to make the bridge aesthetically pleasing for the community, as seen in Illustration 14. To give the bridge similar visual aspects as the Vikingsholm, the foundation piles of the bridge that will extrude from the water will include grey cobble stone on the outside parameter of the piles.

Illustration 14: The Historical Vikingsholm located in Emerald Bay (Emerald Bay State Park, 2017)

Pile Foundations

Pile foundations are needed when the upper soil layers are highly compressible and too weak to support the load added by the superstructure. Piles are primarily used to send the load to the bedrock or to a stronger layer of soil as noted in Figure 15 below.

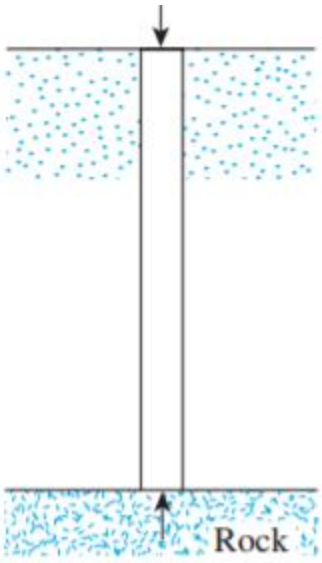

Figure 15: Pile sending load to bedrock (Vesic, 1977)

If bedrock is not encountered at a reasonable depth in the subsurface, piles are incorporated into the design to transmit the structural load to the soil gradually, as noted in Figure 16 below.

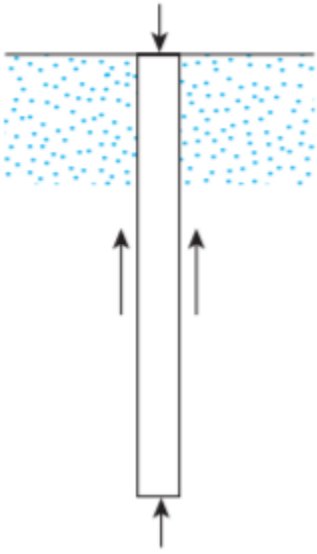

Figure 16: Pile without bedrock (Vesic, 1977)

Pile foundations are also required when there is a high probability of horizontal forces to act on the superstructure. This is because pile foundations can resist bending, while supporting the vertical load that is transmitted by the superstructure (Das, 2007). Since Emerald Bay is located right next to an active fault, piles will be needed in the final design of the proposed bridge. Bridge abutments are also normally built over pile foundations to increase the bearing capacity (Das, 2007).

The type of pile used for a foundation depends on the subsurface conditions, location, how deep the pile must descend below the surface and topography of the area, along with the structural and geometric characteristics of the structure to be supported. There are many different types of piles to consider when designing the bridge foundation including, steel piles, concrete piles, wooden piles and composite piles. The pile type that will be incorporated into the proposed Emerald Bay Bridge will be concrete piles. The category of concrete piles that will be used for the Emerald Bay Bridge are known as precast piles. These piles are prepared using regular reinforcement, the shape will be square for our design, Figure 17 below shows the diagram of the precast square pile with ordinary reinforcement.

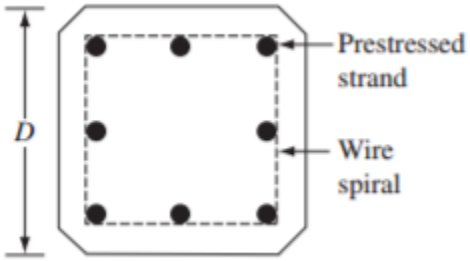

Figure 17: Diagram of the precast square pile with ordinary reinforcement (Vesic, 1977)

The main advantages of concrete piles are that they have a great longevity in most environments, meaning they are corrosion resistant, they are convenient to combine with a concrete structure and can be subjected to hard driving. The main disadvantages of concrete piles are that they are difficult to get a perfect cutoff and they are difficult to transport.

Precast piles can be pre-stressed using high-strength steel pre-stressing cables. The ultimate strength of these cables are around 1,800 $\frac{MN}{m^2}$. While casting the piles, the cables are pre-tensioned to around 900 to 1,300 $\frac{MN}{m^2}$, and the concrete is poured around them. After the curing takes place, the cables are cut, which then produces a compressive force on the pile section. Precast pre-stressed piles usually have a length of 10 meters to 45 meters, the maximum length is 60 meters and the maximum load ranges between 7,500 kN to 8,500 kN.

In the case of point bearing piles, where the bedrock or rocklike material can be found at a reasonable depth, piles can be extended to the rock surface. If a strong layer of soil is the only material that can be found, aside from bedrock, the pile can be extended a few meters into the hard stratum. Figure 18 shows the depth of the piles and the different subsurface components.

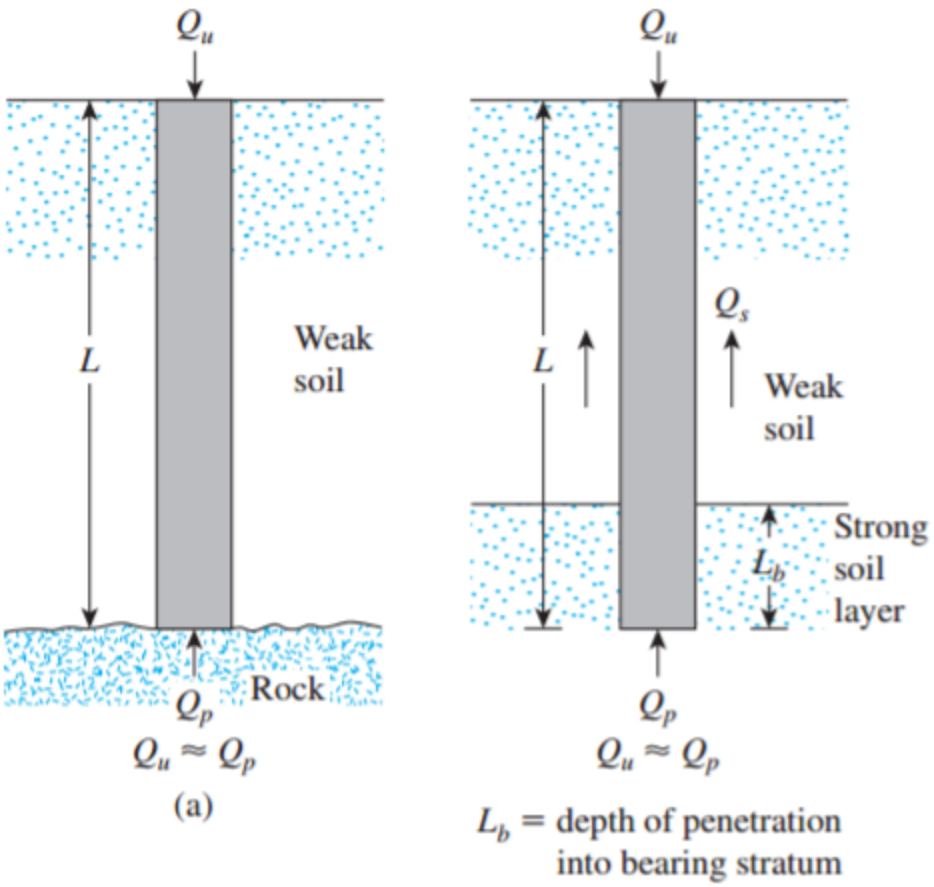

Figure 18: Piles on bedrock or strong soil (Vesic, 1977)

The ultimate load must be considered as well; this is the load that can cause failure of either the pile or soil. The soil will always fail in the same way, where the shear under the point is preceded by direct-shear failure along the shaft. The pile foundations are almost always constructed in groups, each within proximity to one another, the exact distance depending on the stability and the economy of the area.

The ultimate bearing capacity of shallow foundations can be found using Terzaghi's equation for a shallow square foundation as noted in Equation 1. The ultimate bearing capacity was found to be $10{,}079\,\frac{kN}{m^2}$ and then the factor of safety was included

into the calculation to obtain the allowable bearing capacity. This equation can be found in Equation 8, it is $3{,}360\,\frac{kN}{m^2}$. The allowable bearing capacity is per column.

A pile foundation has two components, the first being pile cap and the second being single or group of piles. Figure 19 shows the layout of a pile cap foundation and how the pile is driven into the ground.

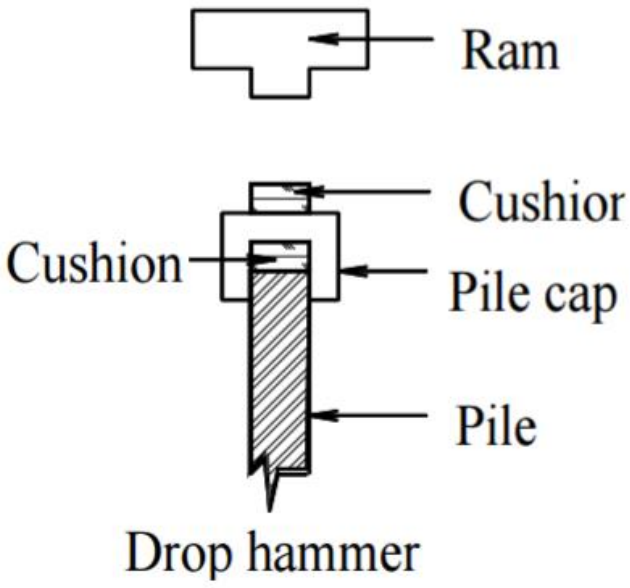

Figure 19: Pile Cap Foundation and Pile Driving (Vesic, 1977)

Pile driving is mainly done by impact hammers, where a ram falls or is repeatedly hit against the pile head (vibratory drivers can also be used). The engineer in charge of driving the piles into the ground must know the computational analysis to calculate the number of blows, the maximum stress in the pile and if a hard or soft cushion should be used. The computational results concluded that both compressive and tensile stresses in the piles can be decreased by using a heavier ram with a lower impact velocity. The stresses can also be decreased using cushions (Vesic, 1977).

Piles should not be used if the driving force causes damage to nearby structures, if the soil has the capability of heaving, or if the area is covered in boulders.

Bridge Style

There are many different styles of bridges that have been used to cross from one side of a mountain or water channel to the other. The bridge types include, but are not limited to, cable-stayed, arch, beam, truss, cantilever, true tied arch and suspension bridges. Each bridge is picked based on the geology of the area, the span needed and the use of the bridge. This is a very important step in designing the type of foundation needed for the proposed Emerald Bay Bridge.

Arch Bridge

Arch bridges are one of the oldest bridge types and have been around for thousands of years due to their natural capability of withstanding large loads. The original design of this style of bridge was stone or brick, which is still used today, but is reinforced with concrete or steel allowing arch bridges to extend in length and have lower spans. The arch of the bridge takes the load and pushes it to the supports at each end of the bridge. These supports, embedded in the ground, are also known as the abutments, which helps keep the bridge from failing. A great example of an arch bridge is the Mike O'Callaghan—Pat Tillman Memorial Bridge that crosses Hoover Dam as seen in Illustration 15 below. This

bridge spans about 1,900 feet. It is a concrete arch bridge topped by a steel deck. Concrete was incorporated into the arch design because it is strong in compression, steel was used as the deck because it is lighter in weight so it lessened the burden of the deck on the arch (Petroski, 2010).

Illustration 15: Mike O-Callaghan—Pat Tillman Memorial Bridge (Hoover Dam Bypass) (Petroski, 2010)

Some advantages of arch bridges include their excellent strength due to their arch design. Due to arch bridges being composed of wedge-shaped stones, the wedge-shaped stones pass the load onto other wedge-shaped stones creating a rippling effect, which eventually will reach the abutments, and then finally the pressure reaches the ground. From here the ground pushes back and the force is eventually pushed back into the wedge-shaped stone locking each stone into place, thus making the bridge stronger each time it is used.

Another advantage of the arch bridge is that it can be made from any kind of material that can withstand pressure. The final advantage is that they are aesthetically pleasing. There are some negatives that come with the arch bridge. One negative is that this bridge is very difficult to build due to the number of factors that need to be considered, along with the time it takes and the large number of workers needed. The arch bridge does have a limited span, the only way to get an arch bridge to cover a large distance is to add multiple arches. They also cannot be built just anywhere; the condition of the ground must be strong and compact enough to support the load that will be distributed along the bridge and all the way down to the abutments. Though it is possible to build on weaker ground depending on the material used. The bridge can be expensive because of the amount of time and labor needed to construct, along with the need of the expertise of many engineers and builders. The materials needed are also expensive. Regular maintenance is also required for the arch bridge because their flexible design makes them more prone to cracking and tearing when exposed to harsh weather.

Final Bridge and Foundation Choice

The arch bridge is the perfect design for the Emerald Bay area. Not only is this style of bridge aesthetically pleasing, but it has a natural capability to withstand large loads. Stone or brick is still the main material used today, but it is now reinforced with concrete or steel making them stronger. Like the Mike O'Callaghan—Pat Tillman Memorial Bridge was built, we will be using concrete in the arch design due to its ability to withstand compression and steel will be used as the deck because it is lighter, giving the arch less of

a burden. Also, steel struts will be used to connect the arch ribs giving the bridge flexibility to protect it during an earthquake (Stillings, 2009).

The pile type that will be used in supporting the bridge are square columns composed of precast concrete that is encased in a thin layer of steel about 5 feet. Each pile will be approximately 40 meters in height along with tub girders that will come in sets of four, that will cover the distance between the columns and support the bridge's deck (Stillings, 2009). For the precast concrete, we will have cobbles dressed around the outside of the columns. The total cost to build the bridge will be estimated around 100 million to 110 million dollars.

Calculations

To find the bearing capacity:

Equation 1: $q_u = c' N_c F_{cs} F_{cd} + q N_q F_{qs} F_{qd} + \frac{1}{2} \gamma B N_\gamma F_{\gamma s} F_{\gamma d}$

$$c' = cohesion$$

$$q = effective\ stress\ at\ the\ level\ of\ the\ bottom\ of\ the\ foundation$$

$$\gamma = unit\ weight\ of\ soil$$

$$B = width\ of\ foundation$$

$$F_{cs}, F_{qs}, F_{\gamma s} = shape\ factors$$

$$F_{cd}, F_{qd}, F_{\gamma d} = depth\ factors$$

$$N_c, N_q, N_\gamma = bearing\ capacity\ factors$$

Calculated:

$$c' = 0.8742$$

$$\gamma = 26\frac{kN}{m^3}$$

$q = \gamma D_f$ →$(D_f = 2B)$→ 2(1.524m) = 3.048m

$$q = \left(26\frac{kN}{m^3}\right) * (3.048m)$$

$$q = 79.25\frac{kN}{m^2}$$

$$B = 1.524m$$

Refer to Appendix B for the bearing capacity factors using $\emptyset = 41°$ (friction angle)

$$N_c = 83.86$$

$$N_q = 73.90$$

$$N\gamma = 130.2$$

Refer to Equations 2, 3 and 4 for the shape factor calculations

$$F_{cs} = 1.034$$

$$F_{qs} = 1.033$$

$$F_{\gamma s} = 0.9848$$

Refer to Equations 5, 6 and 7 for the depth factor calculations

$$F_{cd} = 1.443$$

$$F_{qd} = 1.228$$

$$F_{\gamma} = 1$$

$$q_u = (0.8742)(83.86)(1.034)(1.443) + (79.25)(73.9)(1.033)(1.228) + \frac{1}{2}(26\frac{kN}{m^3})(1.524m)(130.2)(0.9848)(1)$$

$$q_u = 10{,}079\frac{kN}{m^2}$$

To calculate the shape factor:

Equation 2: $F_{cs} = 1 + (\frac{B}{L})(\frac{N_q}{N_c})$

$$F_{cs} = 1 + \left(\frac{1.524m}{40m}\right)(\frac{73.9}{83.86})$$

$$F_{cs} = 1.034$$

Equation 3: $F_{qs} = 1 + \left(\frac{B}{L}\right) tan\emptyset'$

$$F_{qs} = 1 + \left(\frac{1.524m}{40m}\right)\tan(41°)$$

$$F_{qs} = 1.033$$

Equation 4: $F_{\gamma s} = 1 - 0.4(\frac{B}{L})$

$$F_{\gamma s} = 1 - 0.4\left(\frac{1.524m}{40m}\right)$$

$$F_{\gamma s} = 0.9848$$

To calculate the depth factor:

In Radians

Equation 5: $F_{cd} = 1 + 0.4\tan^{-1}(\frac{D_f}{B})$

$$F_{cd} = 1 + (0.4)\tan^{-1}(3.048m/1.524m)$$

$$F_{cd} = 1.443$$

In Radians

Equation 6: $F_{qd} = 1 + 2tan\emptyset'(1 - sin\emptyset')^2 \tan^{-1}(\frac{D_f}{B})$

$$F_{qd} = 1 + 2\tan(41°)(1 - \sin(41°)^2 \tan^{-1}(\frac{3.048m}{1.524m})$$

$$F_{qd} = 1.228$$

Equation 7: $F_\gamma = 1$ (Given)

Calculate the allowable bearing capacity with a factor of safety of 3.

Equation 8: $q_{all} = \frac{q_u}{FS}$

$$q_u = 10{,}079\frac{kN}{m^2}$$

$$FS = 3$$

$$q_{all} = \frac{10{,}079\frac{kN}{m^2}}{3}$$

$$q_{all} = 3{,}360\frac{kN}{m^2}$$

Conclusion

Based on the facts stated throughout the paper, a bridge, cutting across Emerald Bay, would be the best choice when it comes to remediating SR-89. This is primarily due to cost. Building a rock shed would cost approximately 30 to 40 million dollars, but the cost for maintenance would exceed this amount over time. Also, once the rock shed is constructed, there is no way to widen the lanes. If the lanes were to be widened, it would

have to be taken apart and rebuilt increasing the cost to keep the rock shed operating. Whereas the final cost of the bridge will be approximately 110 million to 120 million dollars, and the cost for maintenance would not be as high as the rock shed. The bridge also makes it easy to widen the road, making it a final cost as compared to the rock shed.

Appendix

Bearing Capacity Factors (Das, 2007)

ϕ'	N_c	N_q	N_γ	ϕ'	N_c	N_q	N_γ
0	5.14	1.00	0.00	26	22.25	11.85	12.54
1	5.38	1.09	0.07	27	23.94	13.20	14.47
2	5.63	1.20	0.15	28	25.80	14.72	16.72
3	5.90	1.31	0.24	29	27.86	16.44	19.34
4	6.19	1.43	0.34	30	30.14	18.40	22.40
5	6.49	1.57	0.45	31	32.67	20.63	25.99
6	6.81	1.72	0.57	32	35.49	23.18	30.22
7	7.16	1.88	0.71	33	38.64	26.09	35.19
8	7.53	2.06	0.86	34	42.16	29.44	41.06
9	7.92	2.25	1.03	35	46.12	33.30	48.03
10	8.35	2.47	1.22	36	50.59	37.75	56.31
11	8.80	2.71	1.44	37	55.63	42.92	66.19
12	9.28	2.97	1.69	38	61.35	48.93	78.03
13	9.81	3.26	1.97	39	67.87	55.96	92.25
14	10.37	3.59	2.29	40	75.31	64.20	109.41
15	10.98	3.94	2.65	41	83.86	73.90	130.22
16	11.63	4.34	3.06	42	93.71	85.38	155.55
17	12.34	4.77	3.53	43	105.11	99.02	186.54
18	13.10	5.26	4.07	44	118.37	115.31	224.64
19	13.93	5.80	4.68	45	133.88	134.88	271.76
20	14.83	6.40	5.39	46	152.10	158.51	330.35
21	15.82	7.07	6.20	47	173.64	187.21	403.67
22	16.88	7.82	7.13	48	199.26	222.31	496.01
23	18.05	8.66	8.20	49	229.93	265.51	613.16
24	19.32	9.60	9.44	50	266.89	319.07	762.89
25	20.72	10.66	10.88				

Bibliography

ASTM. (2016). Standard Test Method for Determination of the Point Load Strength Index of Rock and Application to Rock Strength Classifications. *ASTM International.*

Bieniawski, Z.T. (1974). Estimating the strength of rock materials. *Journal of the South African Institute of Mining and Metallurgy*.

Briukhanov, A. V. (1967). On Some New Approaches to the Dynamics of Snow Avalanches.

California Department of Parks and Recreation (2017). *Emerald Bay State Park.* Retrieved from https://www.parks.ca.gov/?page_id=506

Cleaves, A. B. (1960). *Emerald Bay Route Bridge Proposals Correspondence*. Retrieved from EmeraldBayRouteBridgeProposalsCorrespondence

ConnectUS (2015). *Arch Bridges Advantages and Disadvantages.* Retrieved from http://connectusfund.org/arch-bridges-advantages-and-disadvantages-list

Das, Braja (2007). *Principles of Foundation Engineering, SI Seventh Edition.* Retrieved from:http://www.icivilhu.com/Civilteam/4th/Foundations%20Engineering/Principles%20of%20Foundation%20Engineering%207th%20Edition%20SI%20Units.pdf

Design Technology Department. *Arch Bridges – Design Technology.* Retrieved from http://www.design-technology.org/archbridges.htm

Emerald Bay State Park. (n.d.). Retrieved March 10, 2017, from ftp://ftp.consrv.ca.gov/pub/dmg/pubs/sr/SR_230/Notes_LR/CGS_SR230_EmeraldBay_SP_lr.pdf

FDR, (2017). *Central Federal Lands Highway Division of The Federal Highway Administration.* Retrieved from http://www.hdrinc.com/portfolio/mike-ocallaghan-pat-tillman-memorial-bridge-hoover-dam-bypass

Hiroshi. (2007). Rock Fall Sheds - Applications of Japanese Designs in North America.

IIT Gandhinagar. (2017). *Direct Shear Test*. Retrieved from www.iitgn.ac.in/research/stl/directshear.php

Khera, R (14 April 2003). *Pile Example Solution Handout.* Retrieved from http://www.trpa.org/full-road-closure-planned-for-state-route-89-at-emerald-bay-in-september/

Lotshaw, Thomas (16 August 2016). *Full Road Closure Planned for State Route 89 at Emerald Bay in September*. Retrieved from http://www.trpa.org/full-road-closure-planned-for-state-route-89-at-emerald-bay-in-september/

Petroski, Henry (October 2010). *Engineering: Hoover Dam Bypass.* Retrieved from http://www.jstor.org/stable/pdf/27859560.pdf

Schuster, R.L. Krizek, R.J. (1978). *Landslides: Analysis and Control – Special Report 176*. Washington D.C., USA: National Academy of Sciences.

Scott, R.F. Schoustra, J.J. (1968). *Soil Mechanics and Engineering*. USA: McGraw-Hill.

Singh, B. Goel, R.K. (1999). *Rock Mass Classification: A Practical Approach in Civil Engineering*. Oxford, UK: Elsevier Science Ltd.

Vesic, Aleksandar S (1977). *Design of Pile Foundations.* Retrieved from http://www.gnpgeo.com.my/download/publication/L2009_03.pdf